coatings

MDPI

Article

The Influence of CO_2-Cured Incinerated Waste Fly Ash on the Performance of Reactive Powder Concrete

Jianhu Xu [1], Hui Wang [2,*], Wanzhen Wang [2] and Feiting Shi [2]

[1] Zhejiang Institute of Communications, Hangzhou 311112, China
[2] School of Civil Engineering and Geographic Environment, Ningbo University, Ningbo 315215, China; shifeiting@ycit.cn (F.S.)
* Correspondence: wanghui4@nbu.edu.cn

Abstract: Incinerated waste fly ash is a toxic solid, which can cause serious harm to the environment. CO_2-cured incinerated waste fly ash may be useful in decreasing the toxicity of waste fly ash and improving the corresponding mechanical properties of cement-based material with incinerated waste fly ash. Meanwhile, this technology can play a certain role in reducing the content of CO_2 in the atmosphere. In this study, the influence of CO_2-cured incinerated waste fly ash on the rheological parameters (the slump flow and plastic viscosity) and the setting time of fresh reactive powder cement concrete (RPC) is investigated. The flexural and compressive strengths of hardened RPC standard cured for 1 day, 3 days, and 28 days are measured. The leached amounts of Cr and Zn immersed in water for 6 months are measured. The scanning electron microscope photos, thermogravimetric analysis curves, and mercury intrusion curves are obtained. Our results show that the slump flow, the setting time, and the flexural and compressive strengths increased, and the plastic viscosity decreased by adding the waste fly ash with the maximum varying rates of 12.1%, 41.7%, 41.3%, and 61.2%, respectively. CO_2 curing on the waste fly ash can increase the setting time and the flexural and compressive strengths with the maximum varying rates of 19.2%, 13.1%, and 14.2%. The effect of CO_2-cured waste fly ash on the mechanical strengths of RPC is quite limited.

Keywords: CO_2-cured; incinerated waste fly ash; rheological parameters; mechanical properties; scanning electron microscope

Citation: Xu, J.; Wang, H.; Wang, W.; Shi, F. The Influence of CO_2-Cured Incinerated Waste Fly Ash on the Performance of Reactive Powder Concrete. *Coatings* **2023**, *13*, 709. https://doi.org/10.3390/coatings13040709

Academic Editor: Maria Bignozzi

Received: 13 March 2023
Revised: 24 March 2023
Accepted: 30 March 2023
Published: 31 March 2023

1. Introduction

Environmental protection, energy conservation, and the rationality of resources have become important topics in today's society [1,2]. However, with the progress of science and technology, the development of the economy, and the continuous improvement of human material demand, a large amount of domestic garbage has been produced. Traditional domestic waste is incinerated and landfilled [3,4]. The incinerated waste fly ash contains a certain amount of toxic metal elements, which may pollute soil and water [5,6]. A lot of efforts have to be made to solve this problem.

The application of incineration waste fly ash (WFA) in production practice provides ideas for treating this solid waste [7]. Mandpe has confirmed that the WFA can be used in the production of fertilizers [8]. As pointed out in some journals, the WFA possesses a large amount of cementious active substances, which may be advantageous to the mechanical performances of cement-based materials. Ferraro has reported that the lightweight aggregates made from municipal solid WFA through single and double-step pelletization processes show better mechanical strengths than the lightweight aggregates made by clay [9]. The volcanic ash effect of WFA can improve the mechanical strength and the durability of cement concrete [10]. Cui et al. [11] has reported that the reasonable addition (5%~25% by mass ratio of total binder materials) of WFA can improve the mechanical strengths of reactive powder cement concrete (RPC). Meanwhile, the corrosion resistance

of reinforced RPC is increased by mixing the WFA [12]. These things considered, when the RPC with WFA is cured in higher curing temperatures, the mechanical strengths are significantly improved. Even though the incinerated WFA is proven to improve the mechanical strength and corrosion resistance of RPC or other cement-based materials, the problem of toxic release during use has always puzzled many researchers [13]. Based on this reason, methods to reduce the toxicity of WFA need to be developed.

CO_2 curing on raw materials and cement concrete is proven to improve the corresponding mechanical strength [14]. The long-term performances of alkali-activated cementitious materials, magnesium oxysulfate paste, ceramisite cement concrete, and RPC are improved by CO_2 curing [15–17]. The flexural and compressive strengths of RPC are increased to 113.4%~136.1% and 115.8%~141.3% of the standard cured RPC through the use of CO_2 curing for 24 h with the CO_2 concentration of 8% by volume of the total air [18]. Moreover, CO_2 curing can effectively improve the corrosion resistance of the inner steel bars of RPC [19,20]. When CO_2 curing is provided in the RPC, the mechanical strengths' loss rates are 13.1%~25.6%, after 300 NaCl freeze–thaw cycles, while the mechanical strengths' loss rates are 26.8%~37.1% after 30 NaCl dry–wet alternations. However, when the standard curing is provided, the corresponding strengths' loss rates are 33.6%~45.3% and 41.2%~43.8.1% after 300 NaCl freeze–thaw cycles and 30 NaCl dry-wet alternations [21,22]. CO_2 curing is proven to solidify toxic substances in some solid wastes [23]. If CO_2 curing is used in the waste fly ash, the toxicity is likely to be reduced. The CO_2-cured waste fly ash may improve the mechanical properties and reduce the toxicity of raw materials [24,25]. Meanwhile, the application of CO_2 in the WFA provides another way to consume this hazardous gas. However, few journals have reported on this topic.

In this research, the WFA is cured by CO_2 for 24 h. The slump flow, plastic viscosity, and setting time of fresh RPC paste is combined with the WFA, whose mass ratio by the total mass of mineral admixtures are 0%, 25%, 50%, 75%, and 100%, respectively. The corresponding flexural strength, compressive strength, and the drying shrinkage are measured. The scanning electron microscope photos, thermogravimetric analysis curves, and mercury intrusion curves are applied in revealing the mechanism of macro performance. This study will contribute to reducing the content of hazardous waste, reducing exhaust gas pollution, and improving the environment.

2. Experimental Section

2.1. Raw Materials

The granulated blast furnace slag powder (GGBS) and superfine silica fume (SF) were provided by Lingshou County Qiangdong Mineral Products Processing Factory, Shijiazhuan, China. Additionally, the SF showed a specific surface area of 14.8 m^2/g and a density of 2.2 g/cm^3. The density and the specific surface area of the GGBS were 2.91 g/cm^3 and 436.2 m^2/g, respectively. Incinerated waste fly ash manufactured by the Shanghai waste incineration plant was used. The incinerated waste fly ash was obtained after the incineration process. The incinerated waste fly ash (WFA) was cured in the TH-2 concrete carbonization test box with 8% CO_2, which was provided by Shengshi Huike Testing Equipment Co., Ltd., Shanghai, China. The WFA was raw ash, which was directly used after firing. Some WFA was cured in the TH-2 concrete carbonization test box for 1 day. The ordinary Portland (P·O) cement was offered to us by Wenshui County Sunshine Cement Co., Ltd., Luliang, China. P·O cement showed the strength grade of 42.5 MPa, normal cement. The ultrafine Grade I fly ash. provided by Nanjing Hongqian Environmental Protection Engineering Co., Ltd., Nanjing, China, was used in this study. Lingshou Tuolin (Shijiazhuang, China) mineral products processing plant's quartz sands with the particle sizes of 0.68~1.21 mm, 0.33~0.61 mm and 0.14~0.31 mm were used as aggregate in this study. A polycarboxylic water-reducing agent with a water-reducing rate of 40% was used for adjusting the fresh RPC's flowability. Tables 1 and 2 show the chemical composition and particle size distribution of powder materials, respectively.

Table 1. The particle size distribution of the cementitious materials (%).

Types	Particle Size/μm						
	0.3	**0.6**	**1**	**4**	**8**	**64**	**360**
WFA	0.14	0.51	2.3	17.4	31.2	97.3	100
P·O cement	0.1	0.31	2.6	15.1	28.7	93.5	100
GGBS	0.04	0.12	3.3	19.4	35.2	98.2	100
SF	31.3	58.5	82.4	100	100	100	100
Quartz sand	0	0	0	0	0.04	21	100

Table 2. The chemical composition of the cementitious materials (%).

Types	SiO_2	Al_2O_3	Fe_xO_y	MgO	CaO	SO_3	K_2O	Na_2O	Ti_2O	CdO	Cr_2O_3	PbO	CuO	ZnO	Loss on Ignition
WFA	22.4	4.4	0.9	-	20.2	9.56	6	4.3	10.2	0.07	0.09	0.09	0.09	0.5	21.2
P·O cement	20.8	5.6	3.8	1.8	62.1	2.8	-	-	-	-	-	-	-	-	3.1
GGBS	34	14.9	0.5	9.8	36.9	0.3	3.6	-	-	-	-	-	-	-	-
SF	90.8	0.21	0.62	0.23	0.44	0.2	7.5	-	-	-	-	-	-	-	-
Quartz sand	99.8	-	0.2	-	-	-	-	-	-	-	-	-	-	-	-

2.2. Sample Manufacturing

Table 3 shows the mixing proportions of the RPC specimens. All powder materials were put into UJZ-15 and stirred for 30 s. After that, the uniformly mixed solution with a water-reducing agent and water was added and mixed for another 210 s. Once the mixing was finished, the fresh RPC paste was applied in the measurement of the slump flow, plastic viscosity, and yield shear stress. After the measurement of the fresh RPC paste's working properties, the specimens with size of 40 × 40 × 160 mm^3 were prepared for the determination of flexural strength, compressive strength, and drying shrinkage rate. Meanwhile, specimens with a size of 100 × 100 × 100 mm^3 were applied in the measurement of leaching of the toxic metal ions. The manufacturing process of RPC specimens are shown in Figure 1.

Table 3. Mixture design of RPC per one cubic meter (kg).

Water	P·O Cement	WFA	SF	GGBS	Quartz Sand	Water-Reducer
244.4	740.7	0	370.3	111.1	977.9	16.3
244.4	740.7	92.6	277.7	111.1	977.9	16.3
244.4	740.7	185.2	185.2	111.1	977.9	16.3
244.4	740.7	277.7	92.6	111.1	977.9	16.3
244.4	740.7	370.3	0	111.1	977.9	16.3

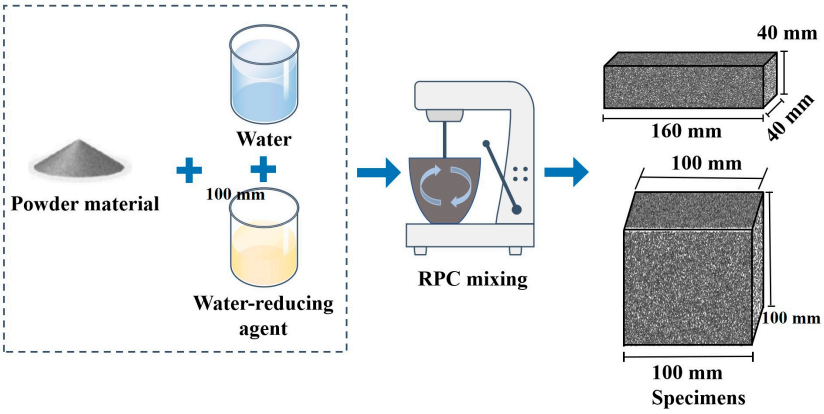

Figure 1. The manufacturing process of RPC specimens.

2.3. Measurement of Basic Performances

The jumping table method is used for measuring the slump flow of the fresh RPC paste. The Brookfield rotational rheometer (Beiying Electronic Technology Co., Ltd., Shanghai, China) was used for testing the plastic viscosity and yield shear stress. ZKS-100 mortar setting time tester (North China Road Construction Instrument, Cangzhou, China) was used to obtain the setting time of fresh RPC paste. The measuring process can refer to Chinese standard JGJ/T70-2009 and references [26–28]. The flexural and compressive strengths of specimens cured in the standard curing environment (temperature of 20 ± 2 °C and relative humility of 98.4%) were tested by carbon material bending and a compression machine provided by Jinan Liling Testing Machine Co., Ltd., Jinan, China. The flexural loading speed and the compressive loading speed were 0.05 kN/s and 2.4 kN/s, respectively. The sample manufacturing and measuring processes are described in GB/T 17671-1999 Chinese standard [29]. The shrinkage rod with an ATORN electronic dial indicator manufactured by Henderson Machinery Technology Co., Ltd., Beijing, China, supporting the middle of one end of the rectangular specimen, was applied in the measurement of dry shrinkage rate. When the specimen's length varied, the value of the length change was read out by the dial indicator. Then, the dry shrinkage rate was obtained. Before the leaching measurement of the toxic metal ions was obtained, specimens were immersed in deionized water for 6 months. The deionized water, immersing the specimens each month, was moved to the RIS Intrepid ER/S ICP atomic emission spectrometer for the measurement of toxic metal ions. In this investigation, the average of six specimens' testing parameters were used in each experiment. Figure 2 shows the measuring process of mechanical strength.

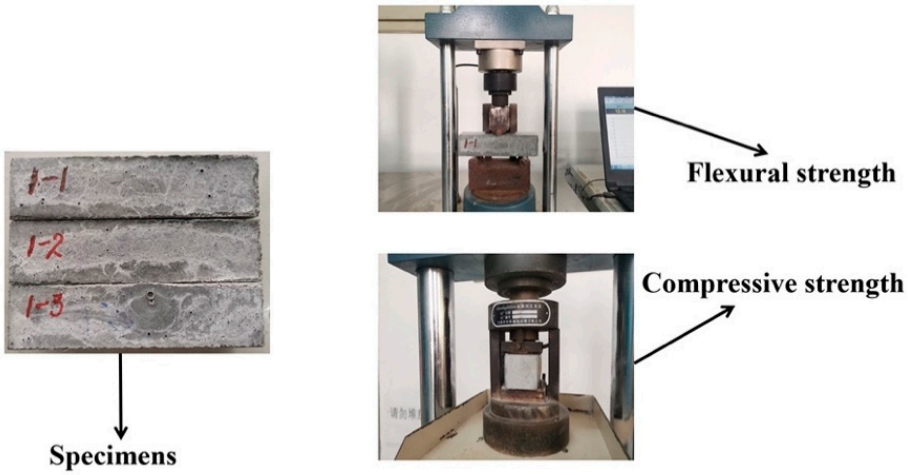

Figure 2. The flexural and compressive strengths of RPC.

2.4. Thermal Analysis and Scanning Electron Microscope

The WFA and the harden RPC specimens with incinerated WFA were prepared for the measurement of the thermogravimetric (TG) analysis and the scanning electron microscope (SEM). Before the TG analysis, all samples were ground into powder and moved to the WCR-123 microcomputer differential thermal analyzer (Beiguang Hongyuan Instrument Co., Ltd., Beijing, China) to obtain the thermogravimetric curves. After being sprayed gold, samples were moved to the FEI Quanta200 field emission scanning electron microscope (Shousi Zhixin Technology Co., Ltd., Beijing, China) in order to acquire SEM photos.

2.5. Mercury Intrusion Analysis

Mercury intrusion curves were obtained by Antonpa mercury intrusion meter provided by Antonpa (Shanghai) Trading Co., Ltd., Shanghai, China. The diameters of the samples used in the experiment ranged from 3.1 to 5.6 mm. The samples were removed from the cores of the specimens.

3. Results and Discussion

3.1. Rheological Parameters and Setting Time of Fresh RPC

Figure 3 shows the slump flow of the fresh RPC. The slump flow of the fresh RPC increased with the increasing dosages of WFA. This was attributed to the fact that the fineness of fly ash was higher than that of the WFA. The fly ash with a larger specific surface area could absorb more free water. Therefore, the slump flow of fresh RPC with WFA was higher. Moreover, the CO_2-cured WFA could decrease the slump flow of fresh RPC due to the fact that the CO_2 can react with alkaline substances in the WFA, forming carbonates, resulting in the reduction of material porosity and increasing the slump flow [30–32].

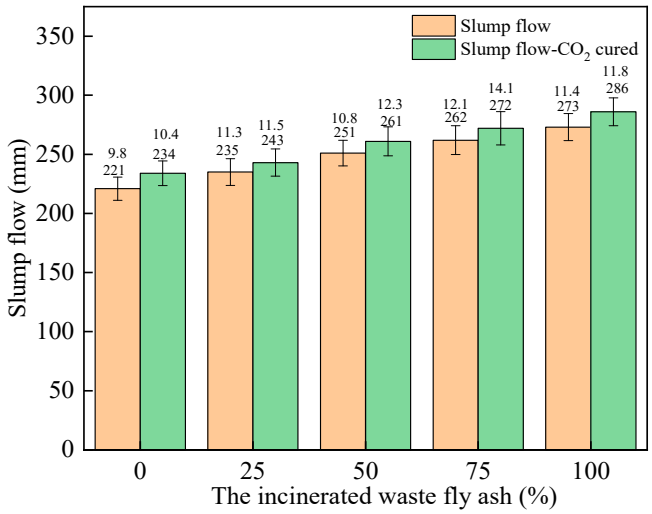

Figure 3. The slump flow of the fresh RPC.

The plastic viscosity of the fresh RPC is shown in Figure 4. The results of the plastic viscosity were the opposite to the fresh RPC's slump flow. The addition of WFA had a reducing effect on the plastic viscosity. Moreover, the CO_2-cured WFA could further decrease the plastic viscosity of fresh RPC. The slump flow of fresh RPC could be increased by WFA with the increasing rates of 10.3%~12.1%. Additionally, the decreasing rates of the plastic viscosity of fresh RPC were 21.7%~47.5%. The increasing rates of slump flow and the decreasing rates of plastic viscosity by CO_2 curing on WFA were 7.8%~11.2% and 13.4%~31.2%.

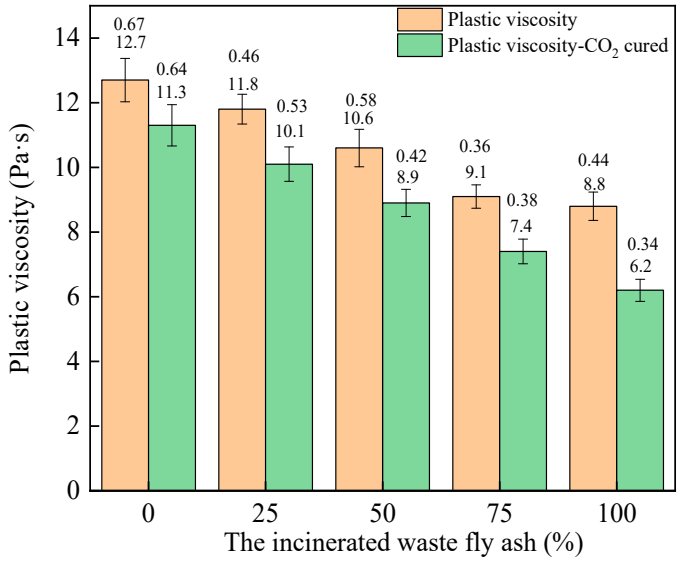

Figure 4. The plastic viscosity of the fresh RPC.

Figure 5 shows the setting time of the fresh RPC. The setting time increased with the increasing dosage of WFA. This was attributed to the fact that the fly ash could absorb a higher dosage of free water than that of WFA, due to the fact that a higher dosage of free water can increase the distance between cement particles and water [33–35]. Therefore, more time was taken to form a skeleton structure, which led to an increase in the setting time. Moreover, as observed in Figure 5, the CO_2-cured WFA can increase the setting time of fresh RPC. This is because CO_2 curing can reduce the pores of WFA, resulting in a higher amount of free water and eventually leading to an increase in the setting time of fresh RPC [36]. The increased rates of setting time, caused by the increased dosage of WFA and the CO_2 curing on WFA were 16.3%~41.7% and 11.3%~19.2%, respectively.

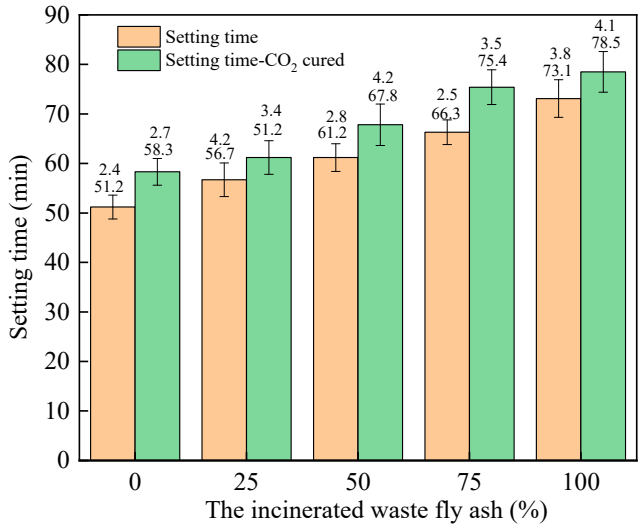

Figure 5. The setting time of the fresh RPC paste.

3.2. Mechanical Performance

The flexural and compressive strengths of RPC with WFA are shown in Figure 6a,b. All specimens were cured for 1 day, 3 days, and 28 days. The flexural and compressive strengths of RPC increased with the curing time, due to the increased hydration degree. The mechanical strengths of RPC were increased by the addition of WFA, which is because the active substances in WFA can promote the secondary hydration of cement, leading to an increase in the hydration degree and the amount and compactness of hydration products, resulting in higher mechanical strength [37,38]. The specimens cured for 1 day show 35.1%~41.3% flexural strengths of the specimens cured for 28 days. Meanwhile, the compressive strengths of specimens cured for 1 day are 48.6%~61.2% of the specimens cured for 28 days.

The mechanical strengths of RPC with CO_2-treated WFA are shown in Figure 6c,d. The flexural strength and compressive strength were increased by adding more CO_2-treated WFA. This was ascribed to the improved secondary hydration of cement by CO_2-treated incinerated WFA [39,40]. The specimens cured for 1 day show 28.3%~39.2% flexural strengths of the specimens cured for 28 days. Meanwhile, the compressive strengths of specimens cured for 1 day are 43.4%~57.1% of the specimens cured for 28 days. Comparing Figure 6c,d with Figure 6a,b, the flexural and compressive strengths of RPC with conventionally treated WFA are 93.1%~97.6% and 91.2%~96.5% of the RPC with CO_2-treated incinerated waste fly ash. This can be ascribed to the forming of carbonate by CO_2 curing, which can reduce the pores of inner incinerated waste fly ash, thus improving the mechanical strengths of RPC [41]. Generally, the increasing effect of CO_2 is inapparent. This may be ascribed to the fact that CO_2 curing can decrease the pores of raw materials, which can improve the mechanical strength [42]. However, the CO_2 curing can reduce the activity of fly ash and garbage fly ash, resulting in strength reduction.

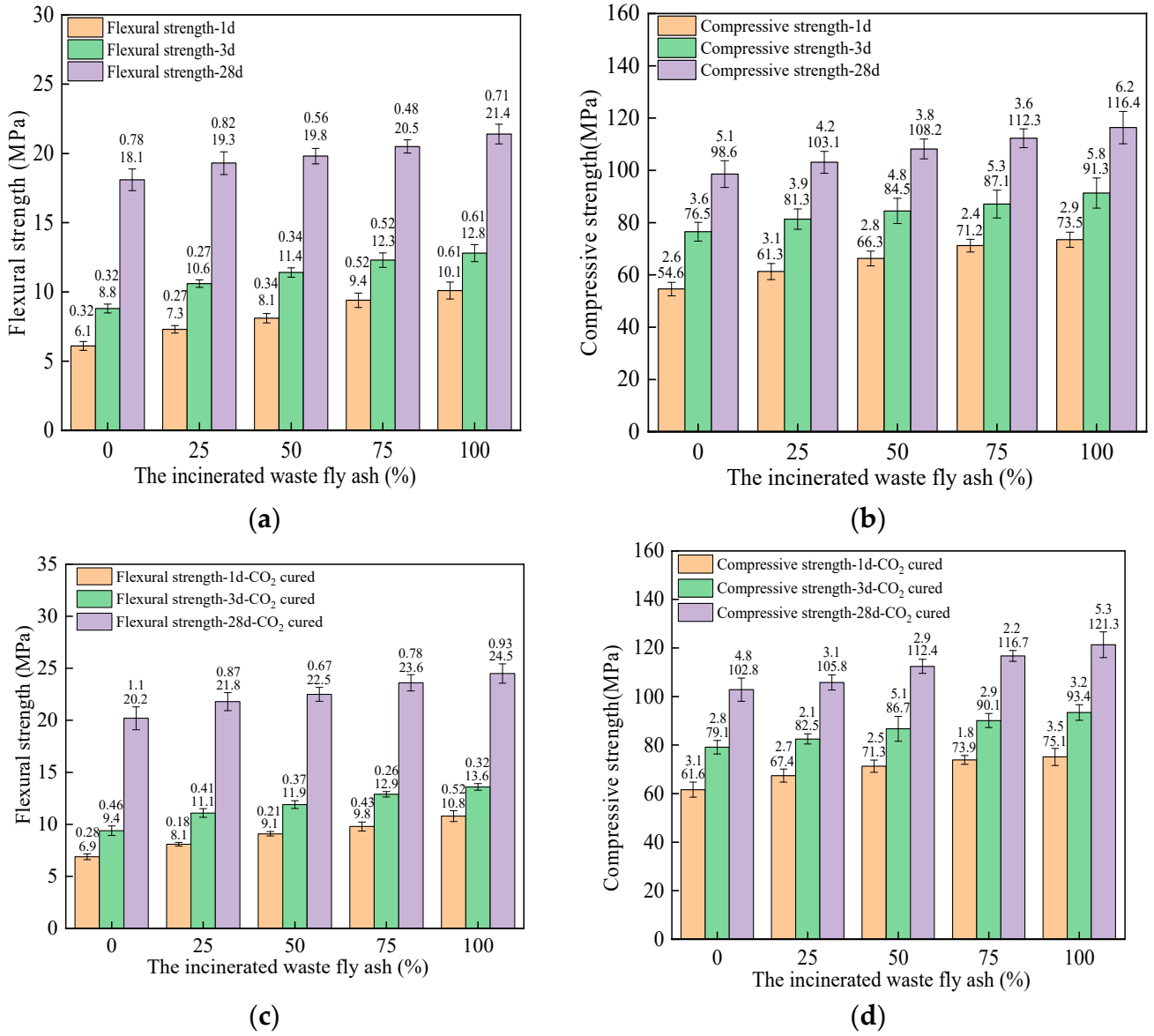

Figure 6. The mechanical strengths of RPC with conventionally treated incinerated waste fly ash. (**a**) Flexural strength. (**b**) Compressive strength. (**c**) Flexural strength. (**d**) Compressive strength.

The increasing rates of mechanical strengths are shown in Figures 7 and 8. As observed in Figures 7 and 8, the increasing rates of mechanical strengths increase with the increasing dosages of WFA and decrease with increased curing age. This is because the WFA can improve the mechanical strengths of RPC. However, the WFA can increase the hydration degree of cement in RPC and the improvement in earlier curing age is higher than that in later curing age [43,44]. Additionally, the increasing rates of mechanical strengths of RPC with CO_2-cured WFA are lower than those of RPC with conventionally WFA, due to the decreased activity of WFA by CO_2 curing [45]. The increasing rates of flexural and compressive strengths of RPC by WFA are 6.6%~65.6% and 4.6%~34.6%.

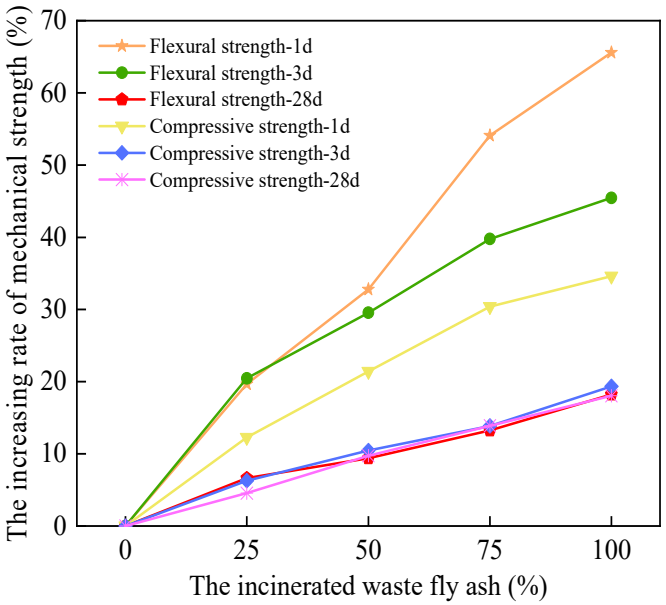

Figure 7. The increasing rates of mechanical strengths of RPC with conventionally treated incinerated waste fly ash.

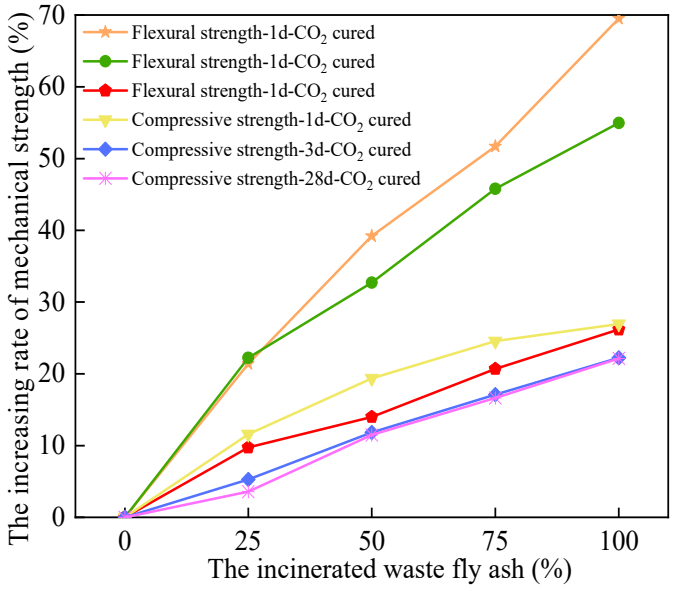

Figure 8. The increasing rates of mechanical strengths of RPC with CO_2 treated incinerated waste fly ash.

3.3. The Leaching of Toxic Metal Elements

Figure 9 shows the leaching amount of toxic metal elements (Cr and Zn). The leaching amount of toxic metal elements increased with the immersing time and the addition of WFA. The CO_2 curing can decrease the leaching amount of toxic metal elements by 76.1% and 71.3%. This is because the WFA contains some toxic metal elements (Cr and Zn), which, when immersed in the water for several months, the toxic metal elements seepage through pores of RPC, thus increasing the content of toxic metal elements [46,47], while the CO_2 curing can decrease the amount of leached toxic metal elements. Comparing Figure 9a with Figure 9b, the amount of leached Zn is higher than that of leached Cr.

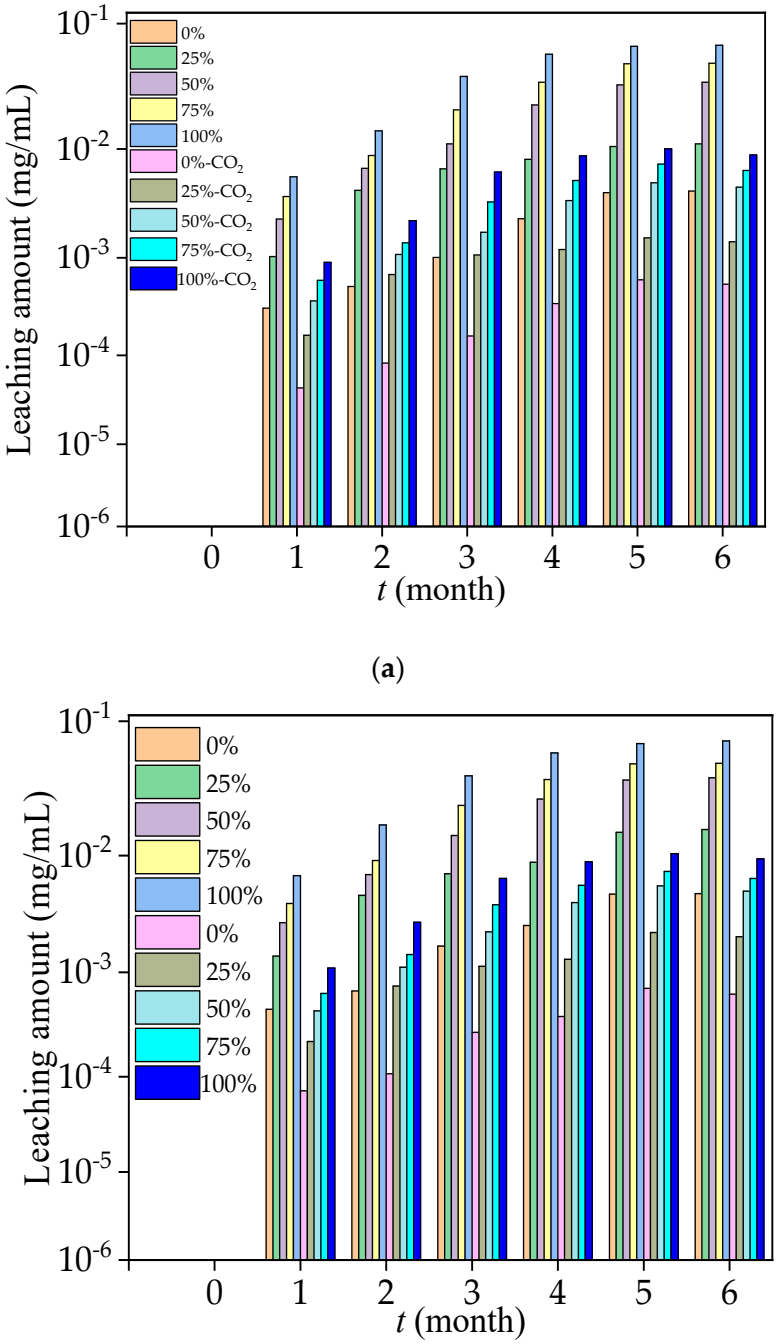

Figure 9. The leaching amount of toxic metal elements. (**a**) The leaching amount of Cr. (**b**) The leaching amount of Zn.

3.4. Microscopic Analysis

Figure 10 shows the thermogravimetric analysis curves of WFA. Moreover, some WFA is CO_2-cured. As observed in Figure 10, the TG decreases in three steps. In the first step (32.03~104.02 °C), the TG obviously decreases. The WFA can absorb some free water in the air. The first reduction of TG is attributed to the evaporation of free water. Meanwhile, as the temperature increases from 104.02 to 581.3 °C, the TG of WFA decreases. The CaO in the incinerated waste fly ash can react with the water in the air, forming $Ca(OH)_2$. The increasing temperature can accelerate the decomposition of $Ca(OH)_2$. Finally, when the

temperature ranges from 581.3 to 712.4 °C, the TG continues to reduce due to the resolved $CaCO_3$, formed by the reaction of $Ca(OH)_2$ and CO_2.

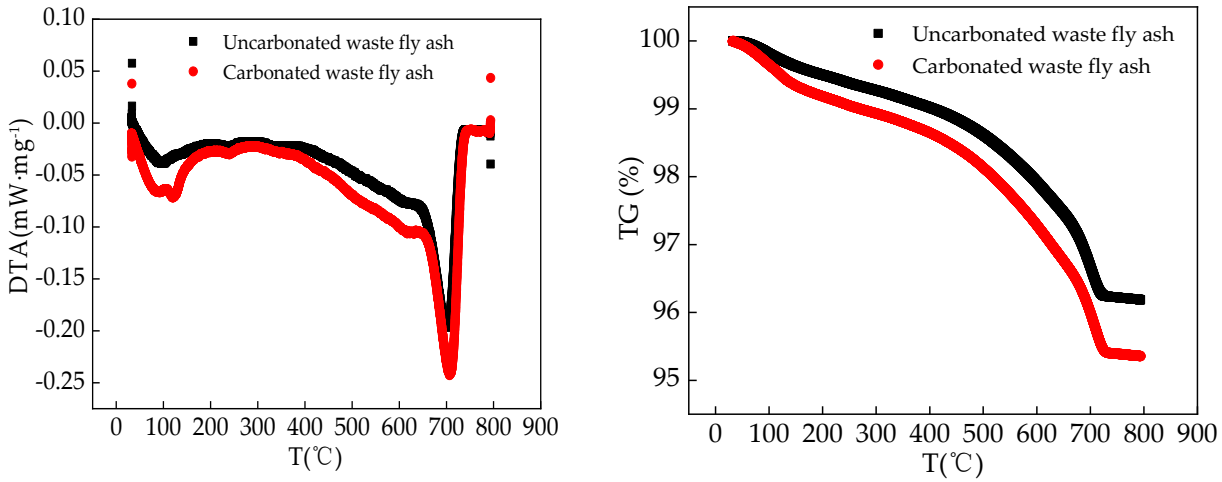

Figure 10. Thermogravimetric analysis curves of incinerated waste fly ash particles.

The SEM photos of WFA particles are shown in Figure 11. As observed from Figure 11, the uncarbonated WFA particle shows smooth particle. However, the carbonated WFA particle shows coarse particles. This is attributed to the formed $CaCO_3$ via the reaction of CaO and CO_2. The $CaCO_3$ absorbs on the surface of the WFA particle, which can prevent the leakage of harmful substances from the WFA.

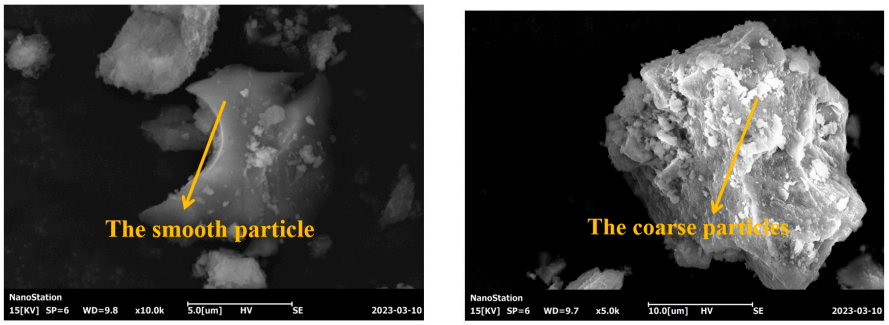

(**a**) (**b**)

Figure 11. The SEM photos of incinerated waste fly ash particles. (**a**) The incinerated waste fly ash particle (**b**) The carbonated incinerated waste fly ash particle.

The SEM photos of RPC with WFA are shown in Figure 12. As observed in Figure 12a, the flocculent hydration product and crack are found in Figure 12a. As shown in Figure 12b, the addition of carbonated WFA has improved the compactness of hydration products, which indicates that the CO_2-cured WFA can increase the mechanical strength by improving the hydration products' compactness. As obtained from Figures 11 and 12, more nanoscale calcium carbonate is generated on the surface of the fly ash after carbonization. This part of calcium carbonate can adsorb cement ions to promote the early hydration of cement and improve early strength. Moreover, the calcium carbonate on the surface of WFA can effectively strengthen the interface between WFA and cement, reducing the formation of cracks. The addition of carbonized WFA reduces the content of rod-shaped hydration products and promotes the transformation of rod-shaped products into dense products. Therefore, the mechanical strengths of RPC are increased by adding the CO_2-cured WFA.

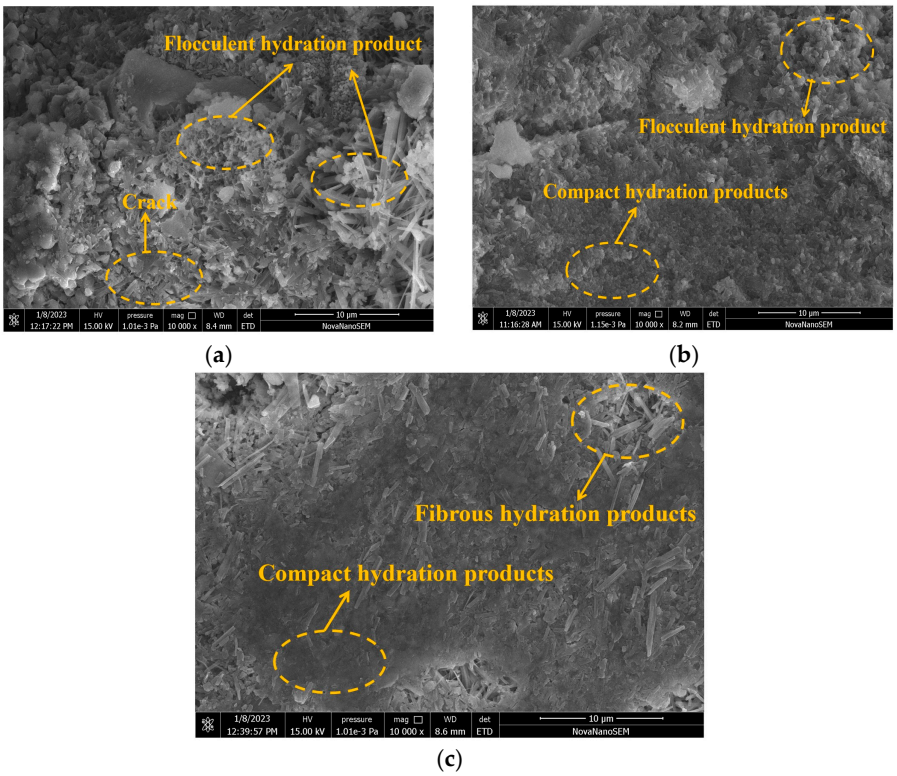

Figure 12. The SEM photos of RPC with incinerated waste fly ash. (**a**) RPC with incinerated waste fly ash (**b**) RPC with 50% carbonated incinerated waste fly ash. (**c**) RPC with 100% carbonated incinerated waste fly ash.

The mercury intrusion curve of RPC with WFA are shown in Figure 13. As illustrated in Figure 13, the main pore diameter of the RPC with WFA ranges from 1.37~4.11 × 10^5 nm. It can be found in Figure 13, that the increase in mass ratio of CO_2-cured WFA leads to a decrease in the total volume of pores (The curve areas can be used to characterize the total volume of pores). Additionally, the increasing dosages of CO_2-cured WFA decrease the volume ratio of pores with a large diameter. These results indicate that CO_2-cured WFA can improve the mechanical strength of RPC.

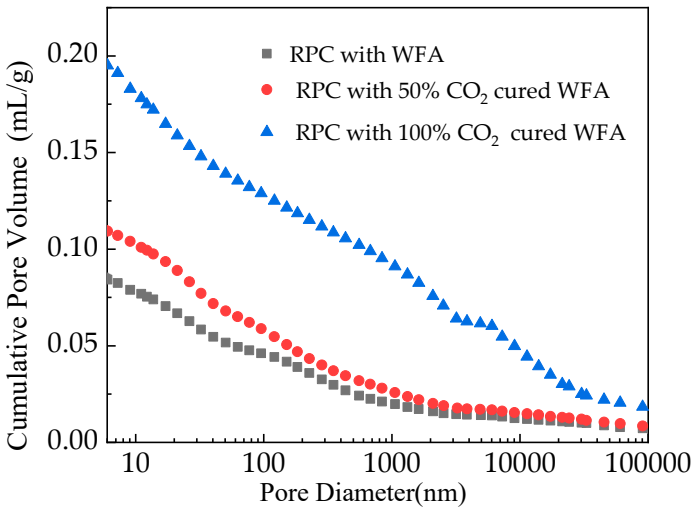

Figure 13. Relationship between pore size and mercury intake.

4. Conclusions

In this study, the influence of incinerated waste fly ash and the corresponding CO_2 curing on the rheological parameters and setting time of fresh RPC are systematically researched. The mechanical properties and intrinsic mechanism are studied. The conclusions can be summarized as follows:

The addition of incinerated waste fly ash can increase the slump flow of fresh RPC with the increasing rates of 10.3%~12.1%. The increasing content of incinerated waste fly ash can lead to decreasing the plastic viscosity with the decreasing rates of 21.7%~47.5%. The mechanical strengths of RPC are improved by adding the incinerated waste fly ash. The increasing rates of incinerated waste fly ash on the mechanical strengths of RPC is decreased by the curing age. The increasing rates of flexural and compressive strengths of RPC caused by incinerated waste fly ash are 6.6%~65.6% and 4.6%~34.6%.

The addition of CO_2-cured incinerated waste fly ash can increase the slump flow and decrease the plastic viscosity with the varying rates of 7.8%~11.2% and 13.4%~31.2%. The addition of incinerated waste fly ash and the effect of CO_2 curing on incinerated waste fly ash can increase the setting time of fresh RPC with the varying rates of 16.3%~41.7% and 11.3%~19.2%. The CO_2-cured incinerated waste fly ash can further improve the mechanical strengths of RPC by decreasing the pore volumes and diameters.

The leaching toxic metal elements (Cr and Zn) are increased with the immersing time, while the amount of Zn is higher than that of the leached Cr. CO_2 curing can decrease the leaching amount of toxic metal elements by 76.1% and 71.3%.

Author Contributions: Conceptualization, H.W. and J.X.; methodology, W.W.; software, H.W.; validation, H.W., J.X. and W.W.; formal analysis, F.S.; investigation, W.W.; resources, H.W.; data curation, J.X.; writing—original draft preparation, H.W.; writing—review and editing, H.W.; visualization, W.W.; supervision, F.S.; project administration, W.W.; funding acquisition, W.W. All authors have read and agreed to the published version of the manuscript.

Funding: The Project of Science and Technology for Public Welfare of Ningbo City (Grant No. 2022S179) and Zhejiang Provincial Natural Science Foundation [LY22E080005].

Institutional Review Board Statement: Not applicable.

Informed Consent Statement: Not applicable.

Data Availability Statement: Not applicable.

Conflicts of Interest: The authors declare no conflict of interest.

References

1. Avila-López, U.; Almanza-Robles, J.M.; Escalante-García, J. Investigation of novel waste glass and limestone binders using statistical methods. *Constr. Build. Mater.* **2015**, *82*, 296–303. [CrossRef]
2. Chen, L.; Wang, Y.; Wang, L.; Zhang, Y.; Li, J.; Tong, L.; Hu, Q.; Dai, J.-G.; Tsang, D.C.W. Stabilisation/solidifification of municipal solid waste incineration fly ash by phosphate-enhanced calcium aluminate cement. *J. Hazard. Mater.* **2021**, *408*, 124404. [CrossRef] [PubMed]
3. Ren, J.; Hu, L.; Dong, Z.; Tang, L.; Xing, F.; Liu, J. Effect of silica fume on the mechanical property and hydration characteristic of alkali-activated municipal solid waste incinerator (MSWI) fly ash. *J. Clean. Prod.* **2021**, *295*, 126317. [CrossRef]
4. Tian, X.; Rao, F.; Morales-Estrella, R.; Song, S. Effects of aluminum dosage on gel formation and heavy metal immobilization in alkali-activated municipal solid waste incineration fly ash. *Energy Fuels* **2020**, *34*, 4727–4733. [CrossRef]
5. Zhang, Y.; Wang, L.; Chen, L.; Ma, B.; Zhang, Y.; Ni, W.; Tsang, D. Treatment of municipal solid waste incineration flfly ash: State-of-the-art technologies and future perspectives. *J. Hazard. Mater.* **2021**, *411*, 125132. [CrossRef] [PubMed]
6. Alderete, N.; Joseph, A.; Van den Heede, P.; Matthys, S.; De Belie, N. Effective and sustainable use of municipal solid waste incineration bottom ash in concrete regarding strength and durability. *Resour. Conserv. Recycl.* **2021**, *167*, 105356. [CrossRef]
7. Xing, J.; Tang, Q.; Gan, M.; Ji, Z.; Fan, X.; Sun, Z.; Chen, X. Co-treatment of municipal solid waste incineration fly ash (MSWI FA) and municipal sludge: A innovative method to improve sludge dewatering with fly ash dichlorination. *J. Environ. Manag.* **2023**, *332*, 117403. [CrossRef]
8. Mandpe, A.; Yadav, N.; Paliya, S.; Tyagi, L.; Yadav, B.R.; Singh, L.; Kumar, S.; Kumar, R. Exploring the synergic effect of fly ash and garbage enzymes on biotransformation of organic wastes in in-vessel composting system. *Bioresour. Technol.* **2021**, *322*, 124557. [CrossRef]

9. Ferraro, A.; Ducman, V.; Colangelo, F.; Korat, L.; Spasiano, D.; Farina, I. Production and characterization of lightweight aggregates from municipal solid waste incineration fly-ash through single and double-step pelletization process. *J. Clean. Prod.* **2023**, *383*, 135275. [CrossRef]
10. Ramesh Kumar, G.; Bharani, S.; Anupriya, R.; Jeevitha, V.; Gnanajothi, G. Influence of electronic waste and fly ash in strength and durability properties of concrete. *Mater. Today Proc.* **2022**, *62*, 2230–2234. [CrossRef]
11. Cui, L.; Wang, H. Influence of waste fly ash on the rheological properties of fresh cement paste and the following electrical performances and mechanical strengths of hardened specimens. *Coatings* **2021**, *11*, 1558. [CrossRef]
12. Cui, L.; Wang, H. Research on the mechanical strengths and the following corrosion resistance of inner steel bars of RPC with rice husk ash and waste fly ash. *Coatings* **2021**, *11*, 1480. [CrossRef]
13. Du, Y.; Hao, W.; Shi, F.; Wang, H.; Xu, F.; Du, T. Investigations of the mechanical properties and durability of reactive powder concrete containing waste fly ash. *Buildings* **2022**, *12*, 560. [CrossRef]
14. Witoon, T.; Numpilai, T.; Nijpanich, S.; Chanlek, N.; Kidkhunthod, P.; Cheng, C.K.; Ng, K.; Vo, D.-V.N.; Ittisanronnachai, S.; Wattanakit, C.; et al. Enhanced CO_2 hydrogenation to higher alcohols over K-Co promoted In_2O_3 catalysts. *Chem. Eng. J.* **2022**, *431*, 133211. [CrossRef]
15. Sharma, R.; Kim, H.; Pei, J.; Jang, J.G. Dimensional stability of belite-rich cement subject to early carbonation curing. *J. Build. Eng.* **2023**, *63*, 105545. [CrossRef]
16. Xu, F.; Chang, R.; Zhang, D.; Liang, Z.; Wang, K.; Wang, H. Improvement of CO_2-cured sludge ceramsite on the mechanical performances and corrosion resistance of cement concrete. *Materials* **2022**, *15*, 5758. [CrossRef] [PubMed]
17. Peng, L.; Yang, J.; Wang, H.; Jin, X. The influence of CO_2 Curing on the mechanical performance and the corresponding chloride ion resistance of alkali-activated compound mineral admixtures. *Coatings* **2022**, *12*, 1920. [CrossRef]
18. Khan, R.I.; Ashraf, W.; Olek, J. Amino acids as performance-controlling additives in carbonation-activated cementitious materials. *Cement Concr. Res.* **2021**, *147*, 106501. [CrossRef]
19. Siddique, S.; Naqi, A.; Jang, J.G. Influence of water to cement ratio on CO_2 uptake capacity of belite-rich cement upon exposure to carbonation curing. *Cem. Concr. Compos.* **2020**, *111*, 103616. [CrossRef]
20. Liang, J.; Zhu, H.; Chen, L.; Qinglin, X.; Ying, G. Rebar corrosion investigation in rubber aggregate concrete via the chloride electro-accelerated test. *Materials* **2019**, *12*, 862. [CrossRef]
21. Ogawa, Y.; Bui, P.T.; Kawai, K.; Sato, R. Effects of porous ceramic roof tile waste aggregate on strength development and carbonation resistance of steam-cured fly ash concrete. *Construct. Build. Mater.* **2020**, *236*, 117462. [CrossRef]
22. Khan, R.I.; Haque, M.I.; Ashraf, W.; Shah, S.; Saleh, N. Role of biopolymers in enhancing multiscale characteristics of carbonation-cured cementitious composites. *Cem. Concr. Compos.* **2022**, *134*, 104766. [CrossRef]
23. Sarmiento, L.E.M.; Clavier, K.A.; Townsend, T.G. Trace element release from combustion ash co-disposed with municipal solid waste. *Chemosphere* **2020**, *252*, 126436. [CrossRef] [PubMed]
24. Song, Z.; Zhang, X.; Tan, Y.; Zeng, Q.; Hua, Y.; Wu, X.; Li, M.; Liu, X.; Luo, M. An all-in-one strategy for municipal solid waste incineration fly ash full resource utilization by heat treatment with added kaolin. *J. Environ. Manag.* **2023**, *329*, 117074. [CrossRef]
25. Lv, Y.; Yang, L.; Wang, J.; Zhan, B.; Xi, Z.; Qin, Y.; Liao, D. Performance of ultra-high-performance concrete incorporating municipal solid waste incineration fly ash. *Case Stud. Constr. Mater.* **2022**, *17*, e01155. [CrossRef]
26. Wong, G.; Fan, X.; Gan, M.; Ji, Z.; Ye, H.; Zhou, Z.; Wang, Z. Resource utilization of municipal solid waste incineration fly ash in iron ore sintering process: A novel thermal treatment. *J. Clean. Prod.* **2020**, *263*, 121400. [CrossRef]
27. *JGJ/T 70-2009*; Standard for Test Method of Basic Properties of Construction Mortar. Ministry of Housing and Urban-Rural Development of the People's Republic of China: Beijing, China, 2009.
28. Zhu, J.; Qu, Z.; Liang, S.; Li, B.; Du, T.; Wang, H. The macro-scopic and microscopic properties of cement paste with carbon dioxide curing. *Materials* **2022**, *15*, 1578. [CrossRef]
29. *GB/T 17671-1999*; Method of Testing Cements-Determination of Strength. The State Bureau of Quality and Technical Supervision: Beijing, China, 1999.
30. Wang, S.; Guo, W.; Bai, Y.; Pan, H.; Qiu, Y.; Xue, C.; Zhao, Q. Preparation and characterization of mortar specimens based on municipal solid waste incineration fly ash-activated slag. *J. Build. Eng.* **2023**, *69*, 106254. [CrossRef]
31. Liu, J.; Wang, Z.; Xie, G.; Li, Z.; Fan, X.; Zhang, W.; Xing, F.; Tang, L.; Ren, J. Resource utilization of municipal solid waste incineration fly ash—Cement and alkali-activated cementitious materials: A review. *Sci. Total Environ.* **2022**, *852*, 158254. [CrossRef]
32. Dong, P.; Liu, J.; Wang, H.; Yuan, H.; Wang, Q. Sustainable municipal solid waste incineration fly ash (MSWIFA) alkali-activated materials in construction: Fabrication and performance. *Nanobuild* **2022**, *14*, 43–52. [CrossRef]
33. Tang, P.; Florea, M.V.A.; Spiesz, P.; Brouwers, H.J.H. Application of thermally activated municipal solid waste incineration (MSWI) bottom ash fines as binder substitute. *Cem. Concr. Compos.* **2016**, *70*, 194–205. [CrossRef]
34. AL-Ameeri, A.S.; ImranRafifiq, M.; Tsioulou, O.; Rybdylova, O. Impact of climate change on the carbonation in concrete due to carbon dioxide ingress: Experimental investigation and modelling. *J. Build. Eng.* **2021**, *44*, 102594. [CrossRef]
35. Smirnov, V.G.; Manakov, A.Y.; Dyrdin, V.V.; Ismagilov, Z.R.; Mikhailova, E.S.; Rodionova, T.V. The formation of carbon dioxide hydrate from water sorbed by coals. *Fuel* **2018**, *228*, 123–131. [CrossRef]
36. Qin, L.; Gao, X.; Chen, T. Influence of mineral admixtures on carbonation curing of cement paste. *Constr. Build. Mater.* **2019**, *212*, 653–662. [CrossRef]

37. Li, Z.; Zhang, W.; Jin, H.; Fan, X.; Liu, J.; Xing, F.; Tang, L. Research on the durability and sustainability of an artificial lightweight aggregate concrete made from municipal solid waste incinerator bottom ash (MSWIBA). *Const. Build. Mater.* **2023**, *365*, 129993. [CrossRef]
38. Liu, B.; Yang, L.; Shi, J.; Zhang, S.; Yalçınkaya, Ç.; Alshalif, A.F. Effect of curing regime on the immobilization of municipal solid waste incineration fly ash in sustainable cement mortar. *Environ. Pollut.* **2023**, *317*, 120839. [CrossRef]
39. Xiang, J.; Qiu, J.; Wang, F.; Li, Z.; Gu, X. Utilization of bioactivated incineration bottom ash in cement binder for mortar harmless treatment and performance improvement. *J. Build. Eng.* **2022**, *57*, 104980. [CrossRef]
40. Tripathy, A.; Acharya, P.K. Characterization of bagasse ash and its sustainable use in concrete as a supplementary binder-A review. *Const. Build. Mater.* **2022**, *322*, 126391. [CrossRef]
41. Matalkah, F. Recycling of hazardous medical waste ash toward cleaner utilization in concrete mixtures. *J. Clean. Prod.* **2023**, *400*, 136736. [CrossRef]
42. Zha, X.; Ning, J.; Saafi, M.; Dong, L.; Dassekpo, J.B.M.; Ye, J. Effect of supercritical carbonation on the strength and heavy metal retention of cement-solidified fly ash. *Cem. Concr. Res.* **2019**, *120*, 36–45. [CrossRef]
43. Ding, Y.; Xi, Y.; Gao, H.; Wang, J.; Wei, W.; Zhang, R. Porosity of municipal solid waste incinerator bottom ash effects on asphalt mixture performance. *J. Clean. Prod.* **2022**, *369*, 133344. [CrossRef]
44. Xie, W.; Li, H.; Yang, M.; He, L.; Li, H. CO_2 capture and utilization with solid waste. *J. Clean. Prod.* **2022**, *3*, 199–209. [CrossRef]
45. Dong, P.; Ding, W.; Yuan, H.; Wang, Q. 3D-printed polymeric lattice-enhanced sustainable municipal solid waste incineration fly ash alkali-activated cementitious composites. *Dev. Built. Environ.* **2022**, *12*, 100101. [CrossRef]
46. Wu, X.; Gu, F.; Su, C.; Wang, W.; Pu, K.; Shen, D.; Long, Y. Preparing high-strength ceramsite from ferronickel slag and municipal solid waste incineration fly ash. *Ceram. Int. Part A* **2022**, *48*, 34265–34272. [CrossRef]
47. Assi, A.; Bilo, F.; Zanoletti, A.; Ponti, J.; Valsesia, A.; La Spina, R.; Zacco, A.; Bontempi, E. Zero-waste approach in municipal solid waste incineration: Reuse of bottom ash to stabilize fly ash. *J. Clean. Prod.* **2020**, *245*, 118779. [CrossRef]